

Measurement of Probe Diffusion in CO₂-Swollen Polystyrene Using in Situ Fluorescence Nonradiative Energy Transfer

Ravi R. Gupta, Vijayakumar S. RamachandraRao, and James J. Watkins*

Chemical Engineering Department, University of Massachusetts, Amherst, Massachusetts 01003

Received October 7, 2002; Revised Manuscript Received December 30, 2002

ABSTRACT: Tracer diffusion coefficients of decacyclene, perylene, and 9,10-bis(phenylethynyl)anthracene (BPEA) in CO₂-swollen polystyrene (PS) films were measured in real time by high-pressure fluorescence nonradiative energy transfer (NRET) using pyrene-labeled polystyrene (PLPS) as the corresponding energy donor. The conditions studied, 55–75 °C and CO₂ pressures between 55 and 104 bar, include regions near and well above the reported glass transition of PS in the presence of CO₂. The diffusivity of the acceptor probes increased markedly upon modest increases in CO₂ sorption. For example, decacyclene diffusivity increased from 6.6×10^{-14} to 1.4×10^{-12} cm²/s as CO₂ sorption increased from 7 to 11 wt %. By comparison to the PS glass at ambient pressure and equivalent temperatures, acceptor probe diffusivities increased by more than 4 orders of magnitude. The concentration dependence of the probe diffusivity is in agreement with the Vrentas–Duda free volume model extended to ternary systems. The analysis indicates that probe diffusion in CO₂-diluted films is strongly coupled to polymer segment mobility, but CO₂ diffusion is not. The friction factor for the probes decreases with decreasing probe volume. The apparent activation energies for decacyclene diffusion in CO₂-diluted films are considerably smaller than those in the PS melt at equivalent values of $T - T_g$.

Introduction

Polymer processing and synthesis using compressible gases and supercritical fluids (SCFs) including carbon dioxide have advanced rapidly in recent years. Because of the poor solubility of most polymers in CO₂, the vast majority of processes using this fluid are heterogeneous. Specific applications include polymer purification and extraction,¹ impregnation of polymer matrices with additives including dyes² and reagents,³ dispersion polymerizations,^{4,5} solid-state polymerizations,^{6,7} polymer modifications, and in situ preparation of polymer composites.^{8–11} In many cases, process dynamics are dictated by transport within a swollen polymer matrix. One role carbon dioxide serves in these applications is that of a benign, transient plasticizing agent. Sorbed CO₂ enhances diffusivities in polymer matrices in analogy to conventional liquid solvents but offers a number of distinct advantages.¹ CO₂ is nonflammable, nontoxic, and environmentally benign and is soluble in and will swell virtually all polymers, including those that are solvent resistant. Moreover, the degree of CO₂ sorption and its solvent quality can be controlled readily by pressure-mediated adjustments in fluid density.¹² Finally, the solvent can be removed from the polymer phase by simple depressurization of the system.

Despite the wide range of emerging applications that exploit supercritical CO₂, there are few studies that quantitatively address the issue of mass transport enhancement in polymer/CO₂ systems. In one early investigation, Berens and co-workers used a simple gravimetric technique to demonstrate that CO₂ accelerates the absorption of small molecule additives including dimethyl phthalate (DMP), 1-butanol, and octane in poly(vinyl chloride) (PVC), polystyrene (PS), and poly(methyl methacrylate) (PMMA) at room temperature.¹³ Increases in diffusivity of up to 6 orders of magnitude

for these penetrants in the polymer matrix upon the sorption of the additive-laden, liquid CO₂ at 25 °C and pressures up to 65 bar were reported. The research groups of Dooley and Cotton each reported enhancements of small molecule diffusion during SCF CO₂ extraction from polymer matrices.^{14,15} Dooley reported an increase of 6 orders of magnitude in the diffusion coefficient of ethylbenzene in CO₂-swollen polystyrene–ethylbenzene mixtures at 50 °C and pressures up to 114 bar. Cotton performed continuous CO₂ extractions of Irganox 1010 (pentaerythritol tetrakis[3-(3,5-di-*tert*-butyl-4-hydroxyphenyl)propionate]) and Irgafos 168 (tris[2,4-ditertiarybutylphenyl] phosphite) from polypropylene using CO₂ at temperatures ranging from 20 to 200 °C and pressures ranging from 100 to 400 bar. Diffusivities of these compounds increased by 2 orders of magnitude over the range of the experiments. More recently, Eckert and co-workers reported an increase in the diffusivity of 4,4'-(diethylamino)nitrobenzene (DENAB) in PMMA in the presence of SC-CO₂ of 2 orders of magnitude at 40 °C as measured by UV–vis spectroscopy.² Each of these studies was limited by the sensitivity of the chosen technique: diffusion coefficients no smaller than 10⁻¹¹ cm²/s can be measured using these approaches. None of the studies examined the dependence of diffusivity on the solvent concentration or probe volume or examined diffusion near T_g .

It is desirable to adapt methods with greater precision and sensitivity such as forced Rayleigh scattering (FRS) and fluorescence nonradiative energy transfer (NRET) to the in situ measurement of diffusion at high pressures. Both techniques have been shown to yield accurate measurement of diffusivities as small as 10⁻¹⁶ cm²/s at ambient pressure. Recently, Paulaitis and co-workers adapted the FRS technique to elevated pressures and measured the tracer diffusion coefficient of azobenzene in PS plasticized by CO₂ at 35 °C and pressures between 14 and 85 bar.¹⁶ Most measurements were taken below T_g where the enhancement in diffu-

* To whom correspondence should be addressed. E-mail: watkins@ecs.umass.edu.

sivity was found to be 2–3 orders of magnitude greater than that predicted on the basis of $T-T_g$ scaling.¹⁶ Data were not obtained at conditions significantly above T_g , namely at higher CO_2 pressures where extensive sorption would severely plasticize the matrix and where most processes are likely to be conducted. Recently, Chapman et al. published results on azobenzene diffusivity in CO_2 -swollen polystyrene at three different temperatures, both above and below the depressed glass transition of CO_2 -polystyrene mixtures.¹⁷ The location of the glass transition temperature depends on the sorbed volume fraction of CO_2 in the polymer. Interestingly, Chapman found that the diffusivities of the azobenzene isomers (*cis* and *trans*) near the glass transition in PS- CO_2 systems exceed that of the polymer melt at equivalent $T-T_g$ scaling. This result suggests that near T_g the sorbed volume of CO_2 plays a role in the probe mobility beyond that predicted on the basis of glass transition depression alone. Our results indicate similar behavior (see Results and Discussion). Finally, Chapman et al. noted differences in diffusion coefficients between the *cis*- and *trans*-azobenzene isomers that were attributed to the differences in the strong attractive interactions between the probes and CO_2 .

Like FRS, fluorescence NRET can be used to accurately determine tracer diffusivities in polymer melts and solutions. One advantage of NRET for studying diffusion is the large number of donor-acceptor pairs known in the literature.¹⁸ Consequently, appropriate probes can be selected to study diffusivity as a function of molecular size, shape, and flexibility among other independent variables.^{19,20} Moreover, probes that do not exhibit strong specific interactions with either CO_2 or the polymer matrix can be chosen. Finally, NRET measurements can be conducted using steady-state fluorescence spectroscopy, which is widely available.

The principles of fluorescence NRET and the framework for their application to the measurement of polymer and probe diffusion have been discussed in detail.^{18,21–27} Recent experiments have validated the approach for polymer melts and polymer solutions at ambient pressure,^{19,28,29} although no previous studies have been conducted at high pressure. Here we adapt NRET for the in situ measurement of small molecule probe diffusion in carbon dioxide-swollen polystyrene films. Specifically, we investigate the concentration, temperature, and size dependence of probe diffusivity at conditions both near and significantly above the glass transition of the polystyrene.

Experimental Section

Decacyclene (Aldrich), perylene (Aldrich), 9,10-bis(phenylethynyl)anthracene (BPEA) (Aldrich), and 1-pyrenylmethyl methacrylate (Polysciences, Inc.) were used as received (Figure 1). CO_2 (Coleman Grade) was used without further purification. Styrene (Aldrich) was extracted with aqueous sodium hydroxide to remove inhibitors and was dried with magnesium sulfate. Polystyrene was synthesized by bulk free radical polymerization. Pyrene-labeled polystyrene was synthesized by bulk free radical copolymerization of 1-pyrenylmethyl methacrylate with styrene. In both cases benzoyl peroxide (Aldrich) was used as the initiator. Molecular weights of the polystyrene homopolymer and copolymer were 240 000 g/mol (PDI = 1.67) and 233 000 g/mol (PDI = 2.2), respectively, as measured by gel permeation chromatography (GPC) calibrated against polystyrene standards. The ratio of pyrene monomer to polystyrene repeat units was approximately 0.009 as determined by UV-vis spectroscopy using Perkin-Elmer

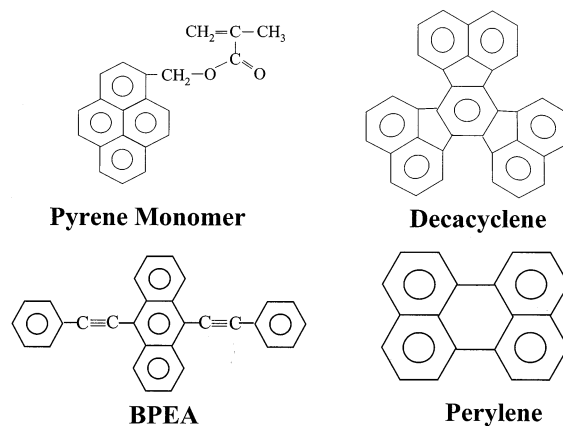


Figure 1. Chromophores used in this study.

Lambda 4c spectrometer. This ratio was further reduced to 0.001 by blending the random copolymer (233K) with the synthesized polystyrene homopolymer (240K). The glass transition temperatures (T_g) of 240K molecular weight polystyrene was 101.5 °C as measured by differential scanning calorimetry (DuPont Instruments DSC2910). The T_g of the copolymer was 102.5 °C. The glass transition temperatures were obtained by extrapolation of data obtained at three different heating rates (2, 5, and 8 °C/min) to zero heating rate. The measured T_g 's are equivalent within experimental error. The concentration of doped chromophore in polystyrene (240K) was 2.78×10^{-3} M. The acceptor doped and pyrene-labeled polystyrene films (PLPS) were spin-coated from toluene solution on a square glass window (1 in. \times 1 in.). The films were dried under vacuum, overnight, at room temperature to remove residual solvent. Films of thickness in the range 0.35–0.72 μm as measured by a Dektak D³ profilometer (Veeco Metrology) were used in this study. Acceptor doped films were floated in a pool of deionized water and transferred on top of a fused quartz disk (1 in. diameter and 1/16 in. thick). The films were annealed under vacuum for 30 min at 130 °C in order to relax the stress developed during the spin-coating process. The polystyrene film sandwich was prepared by floating off the PLPS film in deionized water and transferring it on top of the acceptor-doped polystyrene film. The resulting sample was kept under vacuum at room temperature, overnight, to remove water trapped between the films during the flotation and film transfer steps.

NRET experiments were performed in a custom-built high-pressure stainless steel cell equipped with a high-pressure fiber-optic assembly. The fiber-optic assembly was fabricated using high-pressure tubing, having an outer diameter of 0.25 in. and an inner diameter of 0.125 in. (HIP Inc.) using methods described in the literature.^{30,31} Glass fiber-optic cables with 800 μm core, 830 μm cladding, and numerical aperture (NA) of 0.39 were purchased from Thorlabs. Seven fiber-optic cables, each approximately a meter long, were used to make the assembly. Each cable was stripped of its buffer layer, inserted into the high-pressure tubing, and sealed using JB Weld epoxy. The optical assembly was inserted into the high-pressure cell and sealed with a swagelok 0.24 in. male connector (SS-400-1-2BT, Albany Valve & Fitting Co.) (Figure 2). In situ fluorescence data were obtained using a SPEX Fluoromax-2 spectrometer. The sample was tilted at a slight angle with respect to the excitation beam in order to minimize the amount of reflected incident light from the sample reaching the detector. Three optical fibers were used to carry the incident light from the spectroscopy to the sample, and four fibers were used to capture the fluorescence signal from the sample. The sample size was significantly larger than the incident beam and the region of emanating fluorescence such that only the uniform central part of the sample was interrogated. This precaution eliminates errors introduced by variations in film thickness that result from end effects of the spin-coating step. The cell was housed in an aluminum box filled with glass wool to avoid temperature fluctuations during the experiments. To

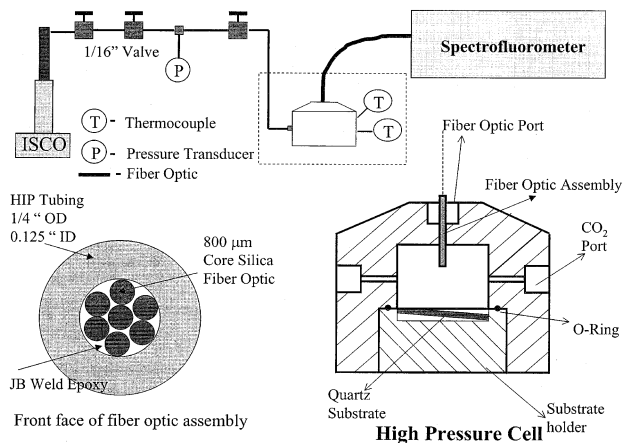


Figure 2. Equipment schematic for high-pressure fluorescence NRET.

facilitate rapid heating, the cell was fitted with four cartridge heaters, controlled within an accuracy of ± 0.5 °C.

Prior to each experiment, the cell containing the sample at ambient pressure was equilibrated at the desired temperature for at least 1 h. At ambient pressure, the temperatures used are well below the T_g of the PS films. CO₂ was then transferred to the cell at a rate of 5–10 mL/min over a period of a few seconds using a computer-controlled syringe pump (ISCO Inc.) equipped with a thermal jacket. Fluorescence emission intensity of the bound pyrene donor was monitored in the time acquisition mode (at 377 nm) using an excitation wavelength of 330 nm. Finally, the value of I_∞ (see eq 1) was measured using a homogeneous sample having an acceptor concentration C_A in both polymer films equal to $C_{A0}[y/(x+y)]$, where y and x are the acceptor and donor film thickness and C_{A0} is the acceptor concentration in the as-cast doped films.

Results and Discussion

A typical experiment involves two polymer films assembled into a sandwich geometry to form an interface. The top film is polystyrene lightly labeled with the fluorescence donor, pyrene, and the bottom film is polystyrene lightly doped with the complementary acceptor such as decacyclene. In this arrangement, the diffusivity of the donor, covalently bound to polystyrene chains, is orders of magnitude below that of the untethered acceptors. As the polymer sandwich is annealed above the glass transition, the acceptors diffuse toward the bound donors, which are assumed to be stationary in the experimental time frame (Figure 3). As the proximity of donor and acceptor molecules increases, a continuous decrease in the observed fluorescence emission intensity of the donor and a complementary increase in the emission intensity of the acceptor are observed due to NRET. Diffusion coefficients of the doped molecule are then calculated from the real-time measurement of the energy-transfer efficiency. Typically, the drop in the donor emission intensity is measured as its quantum efficiency is usually greater than that of the acceptor.

A typical result is shown in Figure 4. The experiment was conducted at 65 °C and a CO₂ pressure of 69 bar, conditions above the glass transition temperature of the polystyrene, which is depressed upon solvent sorption. The spectra show a time-dependent decrease in the emission intensity of the covalently bound pyrene donor that is attributed to the diffusion of decacyclene across the interface. Collection of the full emission spectra is time-intensive (~45 s). The resulting data must be corrected for acquisition time, which leads to uncer-

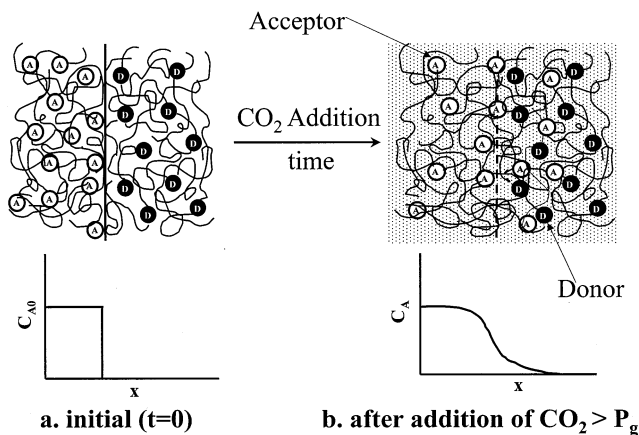


Figure 3. Schematic of the acceptor diffusion in the bilayer film.¹⁹ Sample geometry and concentration profile of the acceptor molecule before (a) after addition of CO₂ (b).

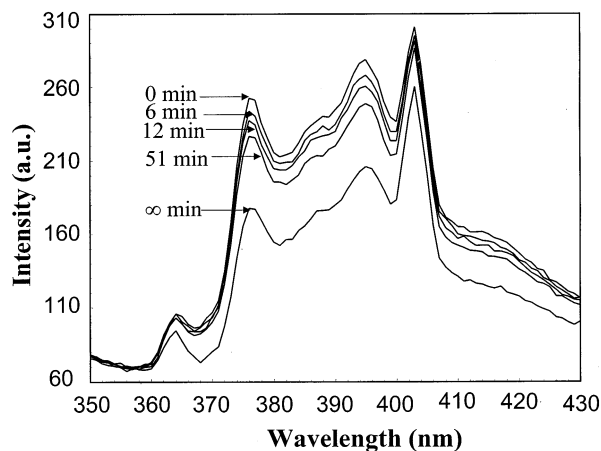


Figure 4. Fluorescence emission spectra of a pyrene-labeled PS/decacyclene-doped PS bilayer film in the presence of CO₂ at 69 bar and 65 °C as a function of annealing time. The emission intensity of the tethered pyrene chromophores decreases as decacyclene diffuses across the interface.

tainities at higher diffusivities. To avoid this problem, all the probe diffusivity data were acquired in the time acquisition mode by following the decrease in pyrene fluorescence intensity at 377 nm. Data collection at a fixed wavelength is quite rapid ($t_{\text{integration}} \sim 0.2$ s), which is required for measuring relatively high diffusivities of acceptor probe in the CO₂-swollen polystyrene. Figure 5 shows the decrease in emission intensity of the pyrene donor as a function of time at 377 nm for diffusion measurements at 65 °C and 69 bar. In all experiments, the film thickness of both acceptor probe-doped polystyrene and pyrene-labeled polystyrene was adjusted such that substantial decreases in emission intensity were measured over experimentally accessible time frames. Diffusion coefficients of acceptor probes were calculated from the data using a system-dependent transport model for the efficiency of energy transfer, $E_N(t)$, via^{19,23}

$$E_N(t) = \frac{E(t)}{E(\infty)} = \frac{I_D(0) - I_D(t)}{I_D(0) - I_D(\infty)} = \left(\frac{\sqrt{D_{\text{probe}} t}}{w} \right) [K_{\text{bn}}] \quad (1)$$

$E_N(t)$ is the normalized energy transfer efficiency, $I_D(0)$, $I_D(t)$, and $I_D(\infty)$ are the corrected experimental fluorescence intensities at the onset of the experiment, the time of interest, and infinite time, respectively,

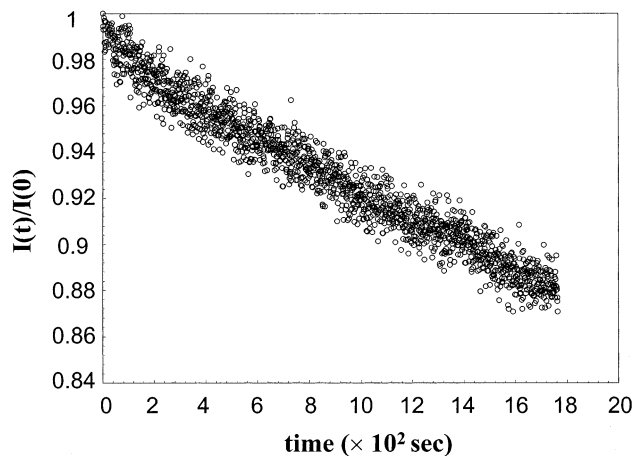


Figure 5. Relative fluorescence emission intensity (377 nm) of pyrene-labeled PS in contact with decacyclene-doped PS as a function of annealing time at 65 °C and 69 bar. The data were obtained in the time acquisition mode, with an integration time of 0.2 s.

D_{probe} is the diffusivity (cm^2/s), t is time in seconds, w is the thickness of the donor-labeled layer, and K_{bn} is given by

$$K_{\text{bn}} = \left(\frac{2\sqrt{\pi} \int_0^{w/(2\sqrt{D_{\text{probe}}t})} a \exp(a^2)(1 - \text{erf}(a)) dy}{\sqrt{\pi}(a_f) \exp(a_f^2)(1 - \text{erf}(a_f))} \right) \quad (2)$$

where

$$a = \frac{C_{A0}}{2A_0}(1 - \text{erf}(y)), \quad y = \frac{z}{2\sqrt{D_{\text{probe}}t}}, \quad a_f = \frac{C_{A0}}{2A_0}$$

C_{A0} is the initial concentration of the doped acceptor in molar units. A_0 is a constant for a given donor–acceptor pair given by

$$A_0 = \frac{3000}{2N_A R_0^3 \pi^{3/2}} \quad (3)$$

where N_A is Avogadro's number and R_0 is the Förster radius in centimeters. The fluorescence emission intensity of the pyrene donor at infinite diffusion time was obtained from an appropriate film as discussed in the Experimental Section. The simple relation (eq 1) between the normalized energy transfer efficiency and tracer diffusivity is derived by assuming Fick's law and is valid only for $t \leq w^2/(16D_{\text{probe}})$.¹⁹ Figure 6 shows the plot of $E_N(t)$ as a function of $t^{1/2}$ for decacyclene and BPEA for representative experiments. The relation between $E_N(t)$ and $t^{1/2}$ is linear in accord with the Fickian assumption for probe mobility in CO_2 -swollen polystyrene matrix. For these examples, the tracer diffusivities of decacyclene at 65 °C and pressures of 69 and 76 bar are 1×10^{-13} and 2.9×10^{-13} cm^2/s , respectively. BPEA diffuses at 6.5×10^{-13} cm^2/s at 65 °C and 76 bar of CO_2 pressure.

Sorption of CO_2 in polystyrene induces dilation of the film and decreases the initial acceptor concentration. These effects must be taken into account in order to accurately determine the probe diffusivity. The volume and weight fraction of CO_2 sorbed in polystyrene and thus the volume change of the polymer film upon CO_2 sorption were calculated using the Sanchez–Lacombe equation of state (S–L EOS) with interaction param-

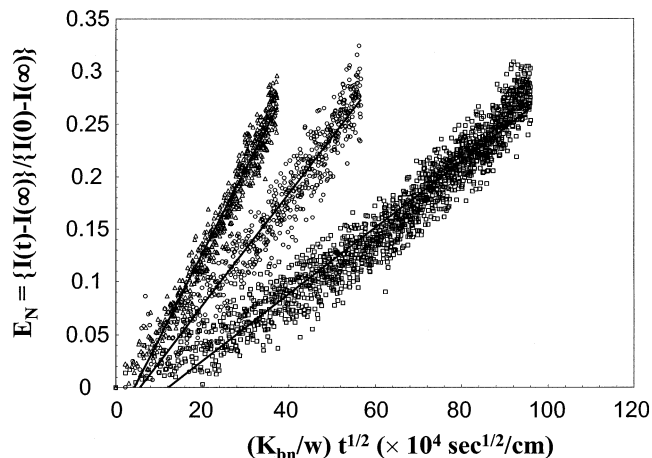


Figure 6. Normalized energy transfer efficiency, $E_N(t)$ vs $t^{1/2}$. Decacyclene in PS– CO_2 at 65 °C and 69 bar (\square), at 65 °C and 76 bar (\circ), and BPEA in the presence of CO_2 at 65 °C and 76 bar (\triangle). The time is normalized with respect to the thickness of the pyrene labeled PS film.

eters obtained by fitting the experimentally determined sorption isotherms. For this purpose we used CO_2 sorption data in PS recently measured by us at 65 °C and pressures between 61 and 102 bar using high-pressure neutron reflectivity.¹² At these conditions, the samples are well above the solvent-depressed glass transition.^{12,32} Details of the calculation are similar to that provided elsewhere.^{33,34} The percent thickness change of the polystyrene films upon CO_2 sorption was assumed to be equal to the percent volume change due to the large surface area-to-thickness ratio of the films.

Figure 7 shows probe diffusivity as a function of weight fraction of CO_2 in the polystyrene matrix. The diffusivity of decacyclene increases by over an order of magnitude at 65 °C upon a modest increase in CO_2 sorption from 7 to 11 wt % (Figure 7a). Similar results were found for isotherms at 55 and 70 °C. By comparison to probe diffusivity at the same temperatures and ambient pressure, conditions under which the polystyrene matrix is a glass, the enhancement in decacyclene diffusivity is more than 4 orders of magnitude. Such behavior clearly demonstrates the effective plasticization of polystyrene matrix by sorbed CO_2 . Similar behaviors were observed for BPEA and perylene probes (Figure 7b). The solid lines shown in the figures are fits using the Vrentas–Duda free volume theory as discussed below.

While the NRET measurements are conceptually straightforward, a number of factors must be considered for application to the measurement of probe diffusion in CO_2 -dilated films. First the chromophores must not leach into the fluid medium. Pyrene is sparingly soluble in CO_2 ,³⁵ but in our experiments this probe was tethered covalently to the PS chains, which are insoluble. The solubilities of the acceptor probes used here in polar and nonpolar solvents are extremely small. Consequently, extraction of acceptor probes into the fluid phase is not anticipated. This was confirmed using fluorescence spectroscopy: no evidence of extraction into a CO_2 phase in contact with a decacyclene-doped PS film at 65 °C and 102 bar was found over a 1.5 h period. Second, as CO_2 sorption in PS increases with pressure, the polarity of the medium changes slightly. Therefore, solvent effects on NRET efficiency and probe emission intensity must be considered. The steady-state emission spectrum of pyrene exhibits several vibrational peaks that are

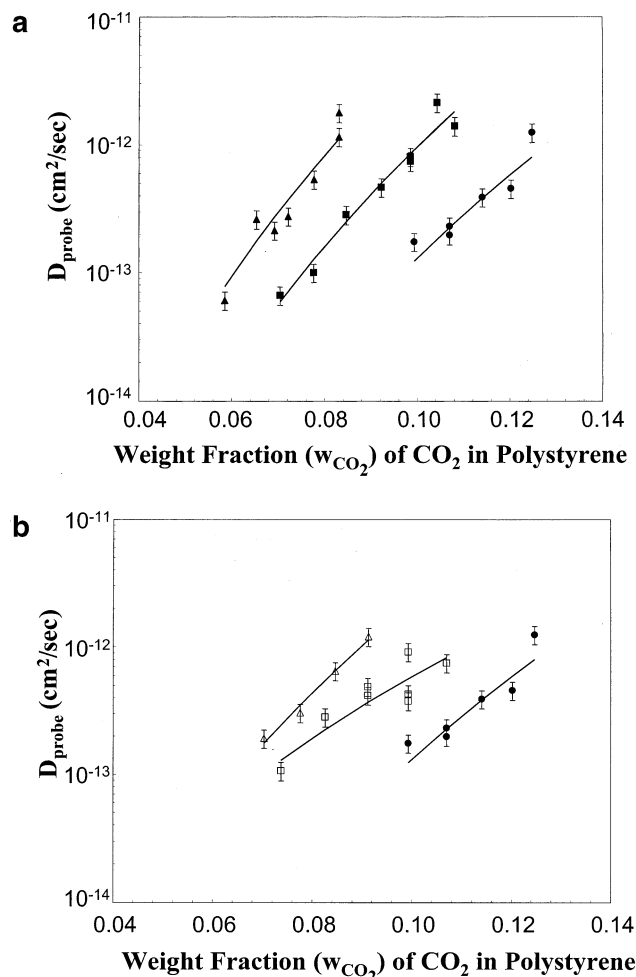


Figure 7. Acceptor probe diffusivity in CO₂-swollen polystyrene as a function of the weight fraction of sorbed CO₂: (A) decacyclene at 55 (●), 65 (■), and 70 °C (▲); (B) BPEA at 65 °C (Δ), perylene at 55 °C (□), and decacyclene at 55 °C (●). The solid lines are fit using the Vrentas–Duda free volume model.

sensitive to the polarity of the medium. For example, the intensity of the 0–0 transition (I_1) is solvent-dependent, but the 0–3 transition (I_3) is insensitive to solvent.³⁵ It is well-known, however, that monosubstituted pyrene derivatives are much less sensitive to solvent polarity than pyrene.³⁶ We found that the emission spectrum of pyrene monomer and pyrene covalently bound to the PS chain was largely insensitive to the medium in which it was distributed: the I_1/I_3 ratio, which characterizes the influence of solvent polarity, remained nearly invariant for both pyrene monomer and pyrene-labeled polystyrene in solutions of chloroform and benzene. Finally, the diffusivity of CO₂ in PS is many orders of magnitude greater than that of probes studied. For example, Arora et al. reported CO₂ diffusivities of 2.4×10^{-6} cm²/s in PS at 80 °C and 238 bar,³⁷ while probe diffusivities reported here are no greater than 10^{-11} cm²/s. Thus, solvent sorption occurs on a time scale that is very short relative to that of the probe diffusion measurements. Therefore, in practice, changes in matrix polarity upon CO₂ sorption have little impact on our measurements. We also assumed that probes tethered to PS chains are essentially immobile in comparison to the more rapidly diffusing doped chromophores. Recently, we reported PS chains diffusivity in CO₂-diluted PS films. Chains of molecular weight 200 000 g/mol exhibit diffusivities

Table 1. Molar Volume (at 0 K), Förster Radius, and Jump Ratios

| | molar vol at 0 K ^a (cm ³ /mol) | | R_0^b (Å) | $\xi_{\text{probe,p}}^c$ | $\xi_{\text{s,p}}^d$ | $\xi_{\text{probe,s}}^e$ |
|-------------|---|------|-------------|--------------------------|----------------------|--------------------------|
| decacyclene | 314 | 36.6 | 1.15 | 0.233 | 4.95 | |
| BPEA | 288 | 33.9 | 1.05 | 0.233 | 4.49 | |
| perylene | 185 | 33.3 | 0.71 | 0.233 | 3.05 | |

^a Molar volume at 0 K calculated from group contribution method of Sugden.⁵² ^b The Förster radius for decacyclene from this study; BPEA and perylene from the literature.¹⁸ ^c Jump ratio from this study. ^d Jump ratio from previous study.³⁸ ^e Jump ratio from eq 6.

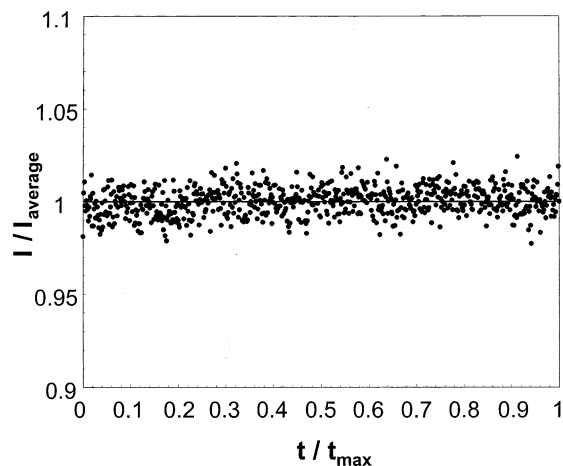


Figure 8. Emission intensity of a pyrene-labeled polystyrene/decacyclene-doped PS bilayer film in the presence of CO₂ as a function of time at 65 °C and 1 bar for 120 min. There is no evidence of pyrene photobleaching.

between 10^{-16} and 10^{-15} cm²/s at 62 °C and pressures between 77 and 104 bar.³⁸ By comparison, the probes investigated in this study exhibit diffusivities between 10^{-13} and 10^{-12} cm²/s at nearly identical conditions.

In principle, the Förster radius is a function of the polarity of medium in which the chromophores are present, since it is determined by the overlap of the absorption and emission spectra of the chromophores. The variation of R_0 with solvent polarity for the acceptor–pyrene pair is, however, quite small. R_0 for decacyclene–pyrene in chloroform, a polar solvent, as determined in this study is 36.6 Å, which is very close to the literature value in benzene, 37.1 Å.¹⁸ The Förster radius values for the acceptor–donor pairs used in this study are listed in Table 1.

It is also necessary to consider the possibility of chromophore photobleaching over the course of the measurements. Figure 8 shows a plot of emission intensity from a bilayer of pyrene-labeled polystyrene film over decacyclene-doped polystyrene film as a function of time at 65 °C and CO₂ pressure of 1 bar. Pyrene emission remains essentially constant, indicating little or no photobleaching of the probes. Finally as mentioned earlier, probe–diluent interactions must be considered. Strong intermolecular interactions between the solvent (or matrix) and the probe can lead to coupling, which affects probe mobility. Strong specific interactions are not expected between CO₂ and the probes used in this NRET study.

The Vrentas–Duda free volume model^{39–41} extended to ternary systems⁴² has been shown to successfully describe the concentration and temperature dependence of probe mobility in polymer solutions.^{20,42–44} The model is based on the theory of Cohen and Turnbull,^{45,46} which

Table 2. Vrentas–Duda Free Volume Parameters^a

| T (°C) | \hat{V}_s^* (cm ³ /g) | V_s^H (cm ³ /g) | \hat{V}_p^* (cm ³ /g) | V_p^H (cm ³ /g) | D_0 |
|-------------------|---------------------------------------|---------------------------------|---------------------------------------|---------------------------------|-----------------------|
| Decacyclene Probe | | | | | |
| 55 | 0.589 | 0.244 | 0.85 | 0.0235 | 0.02 |
| 65 | 0.589 | 0.25 | 0.85 | 0.0239 | 0.088 |
| 70 | 0.589 | 0.257 | 0.85 | 0.0245 | 0.224 |
| BPEA | | | | | |
| 65 | 0.589 | 0.25 | 0.85 | 0.0239 | 0.0194 |
| Perylene | | | | | |
| 55 | 0.589 | 0.244 | 0.85 | 0.0235 | 4.55×10^{-6} |

^a Free volume parameter from previous study,³⁸ except D_0 and $\xi_{\text{probe,p}}$ which are from the Vrentas–Duda model fit to the data.

describes the relationship between diffusion and free volume in a medium of hard spheres. In this study we apply the Vrentas–Duda model to describe the concentration dependence of the probe mobility in CO₂-swollen polystyrene matrices. Recently, we showed that the concentration dependence of polystyrene self-diffusivity correlates well with the Vrentas–Duda theory for binary systems of polystyrene and CO₂.³⁸

The model for ternary systems in the limit of vanishing probe concentration can be written^{20,47}

$$D_{\text{probe}} = D_0 \exp \left[- \frac{\gamma \xi_{\text{probe,p}} \left(\frac{w_s \hat{V}_s^*}{\xi_{s,p}} + w_p \hat{V}_p^* \right)}{\hat{V}_{\text{FH}}} \right] \quad (4)$$

where D_{probe} is the tracer diffusivity of the probe in the polymer solution; D_0 is the preexponential factor, which incorporates the effects of temperature; w_i and \hat{V}_i^* are the weight fraction and the critical hole free volume per gram for the displacement of the i th jumping segment; and s and p denote solvent and polymer, respectively. \hat{V}_{FH} is the average hole free volume per gram of the mixture. If the volume change on mixing is assumed to be small, \hat{V}_{FH} can be obtained by adding the weighted free volume of the respective components of the mixture. γ is the overlap factor signifying that more than one jumping unit can occupy a site. ξ_{ij} is the ratio of the i th and the j th jumping units and is computed using

$$\xi_{ij} = \frac{\hat{V}_i^0(0)M_j}{\hat{V}_j^0(0)M_i} \quad (5)$$

where M_i and M_j are the molecular weights of the i th and j th jumping units; $\hat{V}_i^0(0)$ and $\hat{V}_j^0(0)$ are the specific occupied volume at 0 K. All the parameters are obtained from our previous neutron reflectivity study of PS self-diffusion in CO₂-diluted films³⁸ except D_0 and $\xi_{\text{probe,p}}$, which are used as free fit parameters (see Tables 1 and 2).³⁸ In our study, $T - T_g$ for the polystyrene–CO₂ system ranges from 10 to 40 °C. In this range, the diffusivity in the polymer matrix is free volume limited. Therefore, the temperature dependence of the probe mobility can be absorbed into D_0 , the preexponential term in eq 4, which is then treated as a unified constant.³⁹ We have used D_0 as a fit parameter and have not attempted to attach any additional physical significance. For a more detailed analysis, D_0 must be evaluated over a wide range of temperatures at a constant volume fraction of CO₂ in the polystyrene matrix. The diffusivity data shown in Figure 7a,b are fit to the Vrentas–Duda free volume model using the IMSL library subroutine DB-CLSIF provided in Microsoft Fortran Powerstation (version 4.0).

Insight into solvent and probe diffusion in polymers can be gained by examining the jump ratio ξ_{ij} of the various components in the mixture. Sillescu et al. measured the diffusion coefficient of photoreactive dyes of varying size and flexibility in a number of polymer matrices.⁴⁸ The authors interpreted the jump ratio between probe and polymer, $\xi_{\text{probe,p}}$, as the extent of coupling of the probe mobility to the α -relaxation process above the glass transition temperature. For small probe molecules, solute diffusion does not require cooperative rearrangement of the polymer chains and $\xi_{\text{probe,p}} < 1$. As probe size (volume) increases, the degree of cooperation increases; for full coupling, $\xi_{\text{probe,p}} = 1$. A progressive increase in $\xi_{\text{probe,p}}$ and a ceiling value of 1 are easy to envision when considering diffusion of monomer, oligomers, and polymer chains of increasing molecular weight in a substrate polymer of the same chemical composition. For tracer diffusion of probes having a composition or structure different from the matrix there are other considerations including probe flexibility, shape, and interaction of the probe with the matrix polymer. Nonetheless, after examination of a number of systems, Ehlich and Sillescu proposed that the maximum value of $\xi_{\text{probe,p}}$ is 1 for all species.

Values for $\xi_{\text{probe,p}}$ for decacyclene, BPEA, and perylene obtained in this study are listed in Table 1. For decacyclene, $\xi_{\text{probe,p}}$ is clearly greater than the ceiling value proposed by Sillescu, whereas for BPEA and perylene it is approximately equal to and considerably less than one, respectively. Because of the limited range of probes and solvent concentrations studied, it is difficult to comment definitively on the validity of a ceiling value of 1 for the jump ratio of very large, rigid probes near T_g . However, the value obtained for decacyclene by NRET (1.15) cannot be explained by uncertainty in the measurement alone. This question of a ceiling value for $\xi_{\text{probe,p}}$ will be the subject of future study. Nevertheless, it is clear that the jump ratio decreases with the size of the probe molecule and suggests less coupling of the probe mobility to the segmental relaxation process as the probe size decreases.

The jump ratios between the solvent and the polymer ($\xi_{s,p}$) and the probe and the solvent molecule ($\xi_{\text{probe,s}}$) are related by

$$\xi_{\text{probe,s}} = \frac{\xi_{\text{probe,p}}}{\xi_{s,p}} \quad (6)$$

The results for carbon dioxide and the three probes used in our study are listed in Table 1. The jump ratios suggest that unlike decacyclene, BPEA, or perylene, CO₂ diffusion is not strongly coupled to the α -relaxation of PS. In addition, the jumping units for the probes are considerably larger than that of CO₂; $\xi_{\text{probe,s}} = 4.95, 4.49$, and 3.05 for decacyclene, BPEA, and perylene, respectively.

Wisnudel et al. studied the effect of size, shape, and flexibility on the diffusion of 14 small probes in solutions of low molecular weight PS (3800 g/mol) in tetrahydrofuran (THF), cyclohexane, and carbon tetrachloride solutions of up to 400 g/L using Taylor dispersion and up to 700 g/L using phosphorescence quenching techniques.²⁰ The solvent–polymer jump ratios ($\xi_{s,p}$) for PS in THF,⁴⁹ CCl₄,⁴⁹ and cyclohexane⁵⁰ solution were 0.466, 0.519, and 0.563, considerably greater than the value of 0.233 found for CO₂ dissolved in PS in our study.

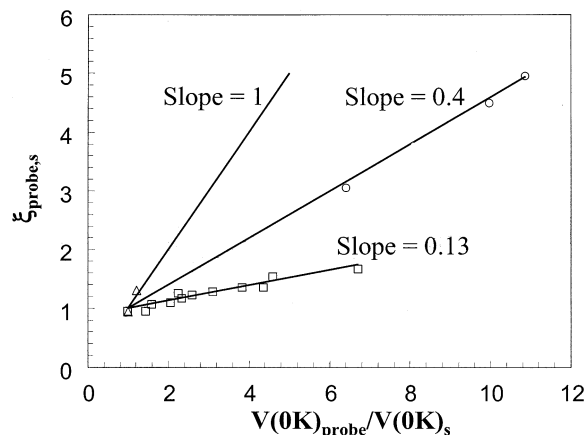


Figure 9. $\xi_{\text{probe},s}$ vs molar volume ratio of probe to solvent at 0 K. Data from Wisnudel et al.²⁰ (Δ , \square); this study (\circ).

There are also differences in the jump ratio of the probe and solvent. If it is assumed that the jump ratio between the probe and the polymer has a ceiling value of 1, as suggested by Sillescu et al., then the largest jump ratio between a probe and THF observed by Wisnudel was 2.14, compared to a value of 4.95 for decacyclene and PS observed in the present study. The latter is close in magnitude to the value for aberchrome 540 determined by Frick et al. in PS–toluene solutions using FRS.⁴⁴ Some, but not all, of these differences can be attributed to differences in the molar volumes of the species involved. Wisnudel found that the $\xi_{\text{probe},s}$ when plotted against the ratio of the molar volumes (at 0 K) of the probe and the solvent molecule either fell on the line with slope 1 or 0.13 and questioned whether these behaviors were universal. A plot of the $\xi_{\text{probe},s}$ vs the ratio of the molar volume of probe to CO₂ at 0 K results in a slope of 0.4 as shown in Figure 9. Results of Wisnudel et al. indicate that $\xi_{\text{probe},s}$ for decacyclene and BPEA in THF at 25 °C fall on the line with slope of 0.13.²⁰ Although the conditions of the two studies are quite different (unentangled chains in solutions vs highly concentrated, high molecular weight systems near T_g), our results suggest that the relationship between $\xi_{\text{probe},s}$ and the molar volumes of the system is not limited to either 1 or 0.13 and is likely system dependent.

Another aim of our study was to obtain the temperature dependence of the friction factor of the probes and compare with the segmental friction factor for polystyrene chains in CO₂-swollen polystyrene matrix. The friction factor for the probe molecules were calculated using the following relation:

$$\xi_{\text{probe}} \sim \frac{T}{D_{\text{probe}}} \quad (7)$$

If the reptation mechanism is valid for polymer chain diffusion in CO₂-swollen polymer matrix, then the segmental friction factor may be calculated using the relation⁵¹

$$\xi_{\text{ps-segment}} \sim \left(\frac{T}{D_s N} \right) \left(\frac{N_e}{N} \right)^{1+\delta} \quad (8)$$

The number of polymer segments for entanglement (N_e) is calculated on the basis of the previous study.³⁸ The exponent δ has a value of 0.26 and is an outcome of the universal molecular weight scaling of the polystyrene

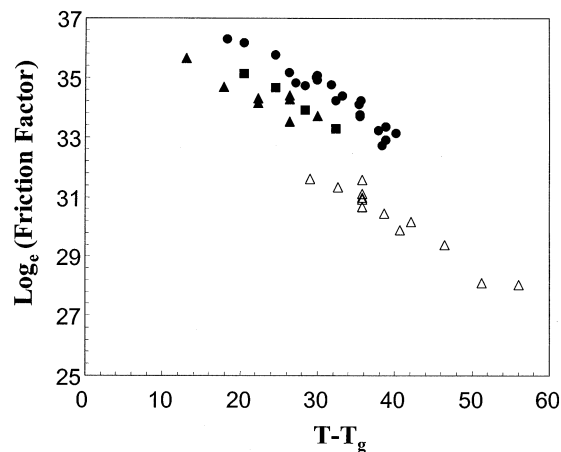


Figure 10. Logarithm of the friction factor vs $T - T_g$ in CO₂-dilated films: decacyclene in PS–CO₂ (\bullet), BPEA in PS–CO₂ (\blacksquare), perylene in PS–CO₂ (\blacktriangle), PS segment friction factor³⁸ (Δ).

self-diffusivity.³⁸ Figure 10 shows the plot of the friction factor with $T - T_g$ in the system. Evaluation of the depression in the glass transition temperature of polystyrene upon sorption of CO₂ is described elsewhere.³⁸ Figure 10 shows that the friction factor for decacyclene is higher than BPEA, which in turn is higher than perylene in concentrated solutions of PS–CO₂. Such a result is in agreement with the Stokes–Einstein equation, which relates the friction factor to the hydrodynamic radius of the molecule. The polystyrene jumping unit, which has the smallest size in this study (108 cm³/mol), has the lowest friction factor. Another interesting outcome from Figure 10 is that decacyclene diffusivity data for the PS/CO₂ system at different temperatures and pressures collapse onto a single curve when scaled with $T - T_g$, which is distinct from the scaling of decacyclene diffusivity in the neat melt. Such a plot may find its utility in predicting probe diffusivity at conditions not easily accessible or outside the limit of a particular technique. Our results are in accord with those of Chapman and Paulaitis, who found azobenzene diffusion in CO₂-dilated PS was substantially more rapid than diffusion in the neat PS melt at equivalent $T - T_g$.¹⁶ While these differences are far in excess of those that could arise from errors in the calculation of T_g , it is important to note that Chapman and we use the same relation to determine T_g depression in CO₂-dilated films.

The apparent activation energy for decacyclene diffusivity in polystyrene swollen matrix was obtained at a constant volume fraction of CO₂ in the polystyrene matrix. Figure 11 shows the apparent activation energies of 57 and 26.5 kcal/mol at CO₂ volume fractions of 0.051 and 0.063 in PS, respectively. The $T - T_g$ in this study ranges from 20 to 40 °C. The apparent activation energy for decacyclene diffusivity in PS melt in the $T - T_g$ range of 3–20 °C is 100 kcal/mol.⁵² The addition of CO₂ lowers the apparent activation energy for the diffusive jump of the probe molecules by increasing the free volume in the system in comparison to the melt in the same $T - T_g$ range.

Conclusions

Fluorescence NRET techniques have been adapted for the measurement of molecular probe diffusion in polymer matrices swollen with supercritical carbon dioxide. In this study, we demonstrated that CO₂ sorption enhances the diffusivity of relatively large organic

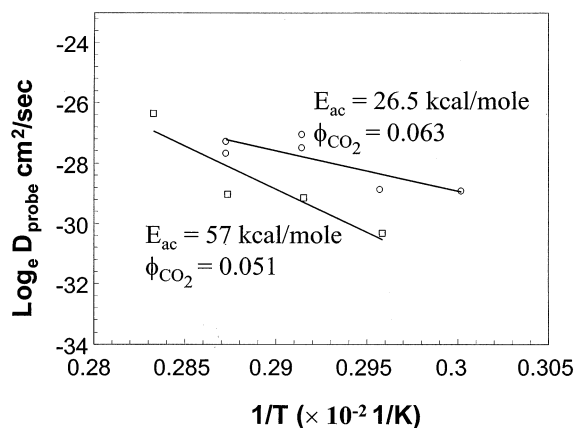


Figure 11. Logarithm of probe diffusivity vs $1/T$. Decacyclene in CO_2 -swollen PS at a volume fraction of 0.051 (\square) and 0.063 (\circ).

acceptor molecules by more than 4 orders of magnitude relative to the PS glass at ambient pressure and the identical temperature. The probe diffusivity increases by over an order of magnitude as sorption of CO_2 in the polystyrene matrix increases from 7 to 11 wt %. Three different probe molecules, varying in volume by a factor of 1.7, were studied. The concentration dependence of the three probes is shown to correlate well with the Vrentas–Duda free volume model extended to ternary systems. The jump ratio between the probe and the polymer segment is shown to decrease with the size of the probes, indicating less coupling of the probe mobility to the relaxation of the polystyrene chain segments as the size of the probe decreases. The jump ratio between the probe and the solvent is much higher than the previous reported ceiling value of 2.14, indicating strong dependence of the ratio on the size and shape of the probe–solvent pair. The ratio is shown to linearly correlate with the volume ratio of the probe to the solvent, at 0 K, with a slope of 0.4. The apparent activation energy of the decacyclene probe in the CO_2 -swollen polystyrene matrix is lower than in the polystyrene melt case in a similar $T-T_g$ range. This indicates the lower friction and thus enhanced diffusivity of the probes in the matrix due to the addition of free volume upon CO_2 sorption.

Acknowledgment. This work was funded by the NSF Material Research Science and Engineering Center at the University of Massachusetts and the David and Lucile Packard Foundation. The authors are also grateful to Prof. Frank Bright and Prof. David Hoagland for suggestions on fluorescence instrumentation and cell design. Helpful suggestions from Prof. John Torkelson regarding NRET and Prof. M. Myrick regarding the high-pressure fiber-optic assembly are also gratefully acknowledged.

References and Notes

- McHugh, M. A.; Krukoni, V. J. *Supercritical Fluid Extraction: Principles and Practice*; Butterworth: Boston, 1986.
- West, B. L.; Kazarian, S. G.; Vincent, M. F.; Brantley, N. H.; Eckert, C. A. *J. Appl. Polym. Sci.* **1998**, *69*, 911–919.
- Howdle, S. M.; Ramsay, J. M.; Cooper, A. I. *J. Polym. Sci., Part B: Polym. Phys.* **1994**, *32*, 541–549.
- DeSimone, J. M.; Maury, E. E.; Menciloglu, Y. Z.; McClain, J. B.; Romack, T. J.; Combes, J. R. *Science* **1994**, *265*, 356–359.
- Adamsky, F. A.; Beckman, E. J. *Macromolecules* **1994**, *27*, 312–314.
- Gross, S. M.; Givens, R. D.; Jikei, M.; Royer, J. R.; Khan, S.; DeSimone, J. M.; Odell, P. G.; Hammer, G. K. *Macromolecules* **1998**, *31*, 9090–9092.
- Gross, S. M.; Roberts, G. W.; Kiserow, D. J.; DeSimone, J. M. *Macromolecules* **2000**, *33*, 40–45.
- Watkins, J. J.; McCarthy, T. J. *Macromolecules* **1994**, *27*, 4845–4847.
- Watkins, J. J.; McCarthy, T. J. *Chem. Mater.* **1995**, *7*, 1991.
- Watkins, J. J.; McCarthy, T. J. *Macromolecules* **1995**, *28*, 4067–4074.
- Brown, G. D.; Watkins, J. J. *Carbon Dioxide-Diluted Block Copolymer Templates for Nanostructured Materials*; MRS Proceedings; 2000; Vol. 584, pp 169–174.
- RamachandraRao, V. S.; Gupta, R. R.; Russell, T. P.; Watkins, J. J. Manuscript in preparation.
- Berens, A. R.; Huvad, G. S.; Korsmeyer, R. W.; Kunig, F. W. *J. Appl. Polym. Sci.* **1992**, *46*, 231–242.
- Dooley, K. M.; Launey, D.; M., B. J.; Caines, T. L. In *Innovations in Supercritical Fluids Science and Technology*; Hutchenson, K. W., Neil, R. F., Eds.; 1994; pp 269–280.
- Cotton, N. J.; Bartle, K. D.; Clifford, A. A.; Dowle, C. J. *J. Appl. Polym. Sci.* **1993**, *48*, 1607–1619.
- Chapman, B. R.; Gochanour, C. R.; Paulaitis, M. E. *Macromolecules* **1996**, *29*, 5635–5649.
- Chapman, B. R.; Paulaitis, M. E. *Macromolecules* **2001**, *34*, 340–342.
- Berlman, I. B. *Energy Transfer Parameter of Aromatic Compounds*; Academic Press: New York, 1973.
- Deppe, D. D.; Dhinojwala, A.; Torkelson, J. M. *Macromolecules* **1996**, *29*, 3898–3908.
- Wisnudel, M. B.; Torkelson, J. M. *Macromolecules* **1996**, *29*, 6193–6207.
- Spangler, L. L. Investigation of Diffusional Processes in Thin Polymer Films Utilizing Novel Fluorescence Techniques. Ph.D. in Chemical Engineering, Northwestern University, 1992.
- Tirrell, M.; Adolf, D.; Prager, S. *Lecture Notes in Mathematics*; Springer-Verlag: Berlin, 1983; Vol. 1063.
- Dhinojwala, A.; Torkelson, J. M. *Macromolecules* **1994**, *27*, 4817–4824.
- Morawetz, H. *Science* **1988**, *240*, 172–176.
- Berlman, I. B. *Handbook of Fluorescence Spectra of Aromatic Molecules*, 2nd ed.; Academic Press: New York, 1971.
- Lakowicz, J. R. *Principles of Fluorescence Spectroscopy*; Plenum Press: New York, 1983.
- Turro, N. J. *Modern Molecular Photochemistry*; The Benjamin Cummings Publishing Co.: San Francisco, CA, 1978.
- Krongauz, V. V.; Mooney, W. F.; Palmer, J. W.; Patricia, J. *J. Appl. Polym. Sci.* **1995**, *56*, 1077–1083.
- Wang, Y.; Zhao, C. L.; Winnik, M. A. *J. Chem. Phys.* **1991**, *95*, 2143–2153.
- Zagrobelyny, J.; Li, M.; Wang, R.; Betts, T. A.; Bright, F. V. *Appl. Spectrosc.* **1992**, *46*, 1895–1897.
- Bell, W. C.; Booksh, K. S.; Myrick, M. L. *Anal. Chem.* **1998**, *70*, 332–339.
- Wissinger, R. G.; Paulaitis, M. E. *J. Polym. Sci., Part B: Polym. Phys.* **1991**, *29*, 631–633.
- RamachandraRao, V. S.; Watkins, J. J. *Macromolecules* **2000**, *33*, 5143–5152.
- Vogt, B. D.; Brown, G. D.; RamachandraRao, V. S.; Watkins, J. J. *Macromolecules* **1999**, *32*, 7907–7912.
- Rice, J. K.; Niemeyer, E. D.; Dunbar, R. A.; Bright, F. V. *J. Am. Chem. Soc.* **1995**, *117*, 5832–5839.
- Dong, D. C.; Winnik, M. A. *Can. J. Chem.* **1984**, *62*, 2560.
- Arora, K. A.; Lesser, A. J.; McCarthy, T. J. *Macromolecules* **1998**, *31*, 4614–4620.
- Gupta, R. R.; Lavery, K. A.; Francis, T. J.; Webster, J. R. P.; Smith, G. S.; Russell, T. P.; Watkins, J. J. *Macromolecules* **2003**, *36*, 346–352.
- Vrentas, J. S.; Duda, J. L. *J. Polym. Sci.* **1977**, *15*, 403–416.
- Vrentas, J. S.; Duda, J. L. *J. Polym. Sci., Polym. Phys.* **1977**, *15*, 417–439.
- Vrentas, J. S.; Duda, J. L. *Macromolecules* **1976**, *9*, 785–790.
- Ferguson, R. D.; von Meerwall, E. D. *J. Polym. Sci., Polym. Phys.* **1980**, *18*, 1285–1301.
- Lodge, T. P.; Lee, J. A.; Frick, T. S. *J. Polym. Sci., Part B: Polym. Phys.* **1990**, *28*, 2607–2627.
- Frick, T. S.; Huang, W. J.; Tirrell, M.; Lodge, T. P. *J. Polym. Sci., Part B: Polym. Phys.* **1990**, *28*, 2629–2649.
- Cohen, M. H.; Turnbull, D. *J. Chem. Phys.* **1959**, *31*, 1164–1169.

- (46) Turnbull, D.; Cohen, M. H. *J. Chem. Phys.* **1961**, *34*, 120–125.
- (47) Huang, W. J.; Frick, T. S.; Landry, M. R.; Lee, J. A.; Lodge, T. P.; Tirrell, M. *AIChE J.* **1987**, *33*, 573–582.
- (48) Ehlich, D.; Sillescu, H. *Macromolecules* **1990**, *23*, 1600–1610.
- (49) Zielinski, J. M.; Duda, J. L. *AIChE J.* **1992**, *38*, 405–415.
- (50) Yu, D. H. S.; Torkelson, J. M. *Macromolecules* **1988**, *21*, 1033–1041.
- (51) Tao, H.; Lodge, T. P.; von Meerwall, E. D. *Macromolecules* **2000**, *33*, 1747–1758.
- (52) Deppe, D. D. Investigation of Small Molecule Diffusion in Thin Polymer Films Using Fluorescence Nonradiative Energy Transfer Technique. Ph.D. in Chemical Engineering, Northwestern University, 1996.

MA021557X